Matrix Isolation Infrared Spectroscopic and Density Functional Study of the Mechanism of the Oxidation of CH_3OH by $CrCl_2O_2$

Bruce S. Ault

Contribution from the Department of Chemistry, University of Cincinnati, Cincinnati, Ohio 45221-0172

Received March 16, 1998

Abstract: The matrix isolation technique has been employed to isolate several intermediates, in sequence, in the oxidation of CH_3OH by $CrCl_2O_2$. Consistent with previous theoretical calculations, a hydrogen-bonded complex formed initially after twin jet deposition and was enhanced by matrix annealing to 33 K. This complex was photodestroyed by Hg arc irradiation with $\lambda < 500$ nm, and led to the production of HCl and $ClCrO_2OCH_3$. These species were also produced by room temperature reaction of the two precursors in a flow system followed by rapid matrix trapping. Heating the flow reaction zone above 150 °C led to destruction of $ClCrO_2OCH_3$, and production of CH_2O and HCl. Above 250 °C bands due to CH_2O were destroyed and bands due to CO and CO_2 grew in. High-level density functional calculations (B3LYP/6-311G*) were carried out to identify potential intermediates in this system and to provide theoretical vibrational spectra for comparison to experiment.

Introduction

High valent transition metal oxyhalide compounds, including chromyl chloride $CrCl_2O_2$, are well-known to serve as potent oxidizing agents for a variety of organic substrates.[1−4] Selective oxidation is important in a range of chemical industries, and numerous studies have sought to determine the mechanism by which these compounds serve as oxidizing agents.[5−10] Nonetheless, many of the mechanistic details have not been well established. These compounds have also been invoked as models for the active sites of a number of metalloenzymes,[11] including cytochrome P-450. In addition, chromyl chloride and a number of CrVI compounds are suspected carcinogens, very likely due to their great oxidizing power. Concurrently, the development of more powerful and sophisticated computers has led to several theoretical studies of the mechanism of reaction of $CrCl_2O_2$ and related compounds with small organic molecules.[12−15] Several of these studies have focused on the reaction of $CrCl_2O_2$ with CH_3OH, calculating pathways and intermediates in the reaction sequence.[16−18] Observation and characterization of these intermediates would contribute substantially to our understanding of these important chemical systems.

The matrix isolation technique[19−21] was developed in the 1950s to facilitate the isolation and characterization of short-lived intermediates. This approach has been applied to the study of diverse species, including radicals, ions, and weakly bound molecular complexes. Recently, a simple flowing gas reactor was coupled to matrix isolation to permit the study of gas-phase bimolecular reactions,[22] with subsequent trapping of the intermediates species in cryogenic matrixes. Very recently, one group reported a study of the photochemical reactions of $CrCl_2O_2$ with olefins in argon matrixes and ethylene oxide in low-temperature solution.[23,24] Also, while the majority of studies of the reactivity of chromyl chloride have been in solution, $CrCl_2O_2$ has substantial vapor pressure and some gas-phase reaction chemistry has been explored.[9,10] Since the flowing gas reactor limits the time available for reaction before matrix deposition, this approach should be appropriate for the study of the intermediates in the reaction of chromyl chloride with small organic substrates. In this study, intermediates and reaction products of the system $CrCl_2O_2 + CH_3OH$ are reported.

Experimental Section

All of the experiments in this study were conducted on conventional matrix isolation apparatus that has been described.[25] In the flowing gas reactor, referred to as merged jet deposition,[22] the two gaseous

(1) Hartford, W. H.; Darrin, M. *Chem. Rev.* **1958**, *58*, 1.
(2) Sharpless, K. **B.**; Teranishi, A. Y.; Backvall, J.-E. *J. Am. Chem. Soc.* **1977**, *99*, 3120.
(3) Freeman, F.; McCart, P. D.; Yamachika, N. J. *J. Am. Chem. Soc.* **1970**, *92*, 4621.
(4) Scott, S. L.; Bakac, A.; Espenson, J. H. *J. Am. Chem. Soc.* **1992**, *114*, 4205.
(5) Westheimer, F. H.; Chang, Y. W. *J. Phys. Chem.* **1959**, *63*, 438.
(6) Wiberg, K. **B.**; Eisenthal, R. *Tetrahedron* **1964**, *20*, 1151.
(7) Necsoiu, I.; Balaban, A. T.; Pascaru, I.; Sliam, E.; Elian, M.; Nenitzescu, C. D. *Tetrahedron* **1963**, *19*, 1133.
(8) Freeman, F.; Arledge, K. W. *J. Org. Chem.* **1972**, *37*, 2656.
(9) Cook, G. K.; Mayer, J. M. *J. Am. Chem. Soc.* **1994**, *116*, 1855.
(10) Cook, G. K.; Mayer, J. M. *J. Am. Chem. Soc.* **1995**, *117*, 7139.
(11) Sharpless, K. **B.**; Flood, T. C. *J. Am. Chem. Soc.* **1971**, *93*, 2316.
(12) Rappe, A. K.; Goddard, W. A., III *J. Am. Chem. Soc.* **1980**, *102*, 5114.
(13) Rappe, A. K.; Goddard, W. A., III *J. Am. Chem. Soc.* **1982**, *104*, 448.
(14) Rappe, A. K.; Goddard, W. A., III *J. Am. Chem. Soc.* **1982**, *104*, 3287.
(15) Rappe, A. K.; Goddard, W. A., III *Nature* **1980**, *285*, 311.
(16) Ziegler, T.; Li, J. *Organometallics* **1995**, *14*, 214.
(17) Deng, L.; Ziegler, T. *Organometallics* **1996**, *15*, 3011.
(18) Deng, L.; Ziegler, T. *Organometallics* **1997**, *16*, 716.
(19) Hallam, H. E. *Vibrational Spectroscopy of Trapped Species*; John Wiley and Sons: New York, 1973.
(20) Craddock, S.; Hinchliffe, A. *Matrix Isolation;* Cambridge University Press: Cambridge, 1975.
(21) *Chemistry and Physics of Matrix Isolated Species*; Andrews, L., Moskovitz, M., Eds.; Elsevier Science Publishers: Amsterdam, 1989.
(22) Limberg, C.; Koppe, R.; Schnockel, H. *Angew. Chem., Int. Ed. Engl.* In press.
(23) Limberg, C.; Cunskis, S.; Frick, A. *J. Chem. Soc., Chem. Commun.* **1998**, 225.
(24) Carpenter, J. D.; Ault, **B.** S. *J. Phys. Chem.* **1991**, *95*, 3502.
(25) Ault, B. S. *J. Am. Chem. Soc.* **1978**, *100*, 2426.

S0002-7863(98)00875-0 CCC: $15.00
Published on Web 06/06/1998

reactants, each diluted in argon, were prepared in separate gas-handling manifolds. The two deposition lines were then joined with an Ultratorr tee at a distance from the cryogenic surface, and the flowing gas samples were permitted to mix and react during passage through the merged region. The length of this region was variable, from 10 to 300 cm. In addition, the merged region could be heated to as high as 400 °C, to induce further reaction. The flowing gas mixture exited the tip of the deposition line and was sprayed onto the 14 K cold surface for 20−24 h before final infrared spectra were recorded either on a Bruker 113v or a Perkin-Elmer Spectrum 2000 Fourier transform infrared spectrometer at 1 cm^{-1} resolution. Additional experiments were conducted in the twin jet mode, where the two reactants, each diluted in argon, were co-deposited on the cold surface from separate nozzles. A number of these matrixes were subsequently warmed to 33−35 K to permit annealing and limited diffusion, and then recooled to 14 K and additional spectra recorded. Also, many of these matrices were irradiated with the filtered output of a medium-pressure Hg arc after which additional spectra were recorded.

Chromyl chloride (Aldrich) was introduced into the vacuum system as the vapor above the room-temperature liquid, after purification in a glass finger by freeze−pump−thaw cycles. CH_3OH (Aldrich), CD_3OH, CD_3OD, $^{13}CH_3OH$, and CH_318OH (all Cambridge Isotope Laboratories, 99% isotopic enrichment) were also introduced as the vapor above the room-temperature liquid, after repeated freeze−pump−thaw cycles. In several experiments, CH_2O was employed as a reactant; this species was produced by sublimation of solid paraformaldehyde $(CH_2O)_x$ at approximately 50 °C from a metal finger attached to the deposition line. In a few experiments, HCl (Matheson) was employed as a reactant after introduction into the vacuum system from a lecture bottle and purification by freeze−pump−thaw cycles at 77 K. Argon was used as the matrix gas in all experiments, and was used without further purification.

Ab initio calculations were conducted on the likely intermediate species in this study, using the Gaussian 94 suite of programs.[26] Both restricted Hartree−Fock and density functional calculations employing the Becke functional B3LYP were conducted to locate stable minima, determine structures, and calculate vibrational spectra. Final calculations with full geometry optimization employed the 6-311G* triple-ζ basis set, after initial calculations with smaller basis sets were run to approximately locate energy minima. Calculations were carried out on a Silicon Graphics Indigo 2 workstation.

Results

Blank experiments were carried out in the twin jet mode for each of the reagents alone in argon prior to any co-deposition experiments. The spectra obtained were in good agreement with literature spectra.[27−33] Several of these blank experiments were subsequently annealed to around 34 K, recooled, and scanned. Some aggregation was noted in spectra of CH_3OH samples, while no distinct changes were noted in spectra of $CrCl_2O_2$ samples. A blank experiment of each reagent was also irradiated with the Pyrex/H_2O-filtered output of a medium-pressure Hg arc lamp. No changes were seen as a result of irradiation. In addition, blank experiments were conducted in the merged jet mode with the merged region heated to as high as 380 °C, for comparison to the merged jet pyrolysis experiments. The spectra of $Ar/CrCl_2O_2 = 100$ samples after pyrolysis to 380 °C were unchanged relative to deposition through a room-temperature line. In contrast, there was some evidence of decomposition of Ar/CH_3OH samples above 300 °C, leading to the production of CH_4, CO, and CO_2 in the matrix. There was no evidence of decomposition of Ar/CH_2O samples during high-temperature pyrolysis.

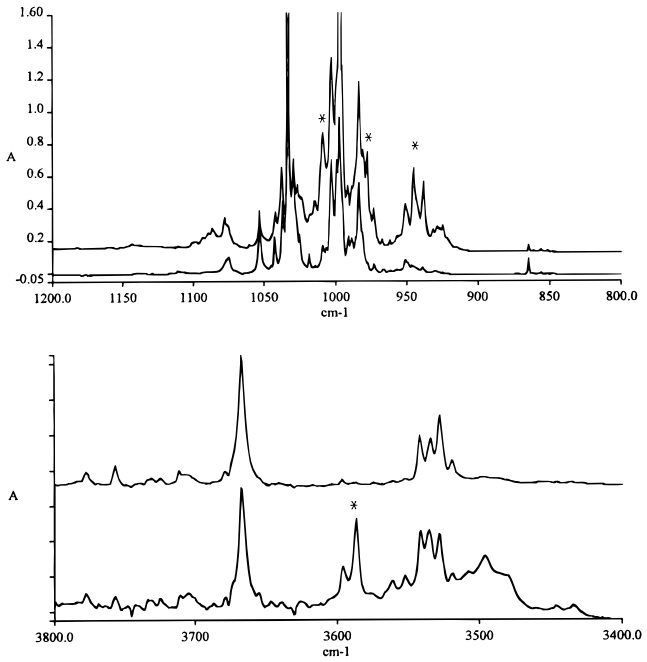

Figure 1. Infrared spectra over selected spectral regions of matrixes prepared by twin jet deposition of samples of $Ar/CrCl_2O_2 = 100$ and $Ar/CH_3OH = 250$. The upper trace was taken before annealing while the lower trace was taken after annealing to 33 K and recooling to 14 K. Bands denoted by an asterisk are attributable to species **A**.

$CrCl_2O_2$ + CH_3OH. (a) Twin Jet Experiments. The reaction chemistry of these two compounds was initially explored in a twin jet experiment in which a sample of $Ar/CrCl_2O_2 = 100$ was co-deposited with a sample of $Ar/CH_3OH = 250$. The resultant spectrum showed intense bands due to the two parent species, along with a set of very weak new absorptions at 429, 443, 944, 978, 1010, 1313, 3586, and 3596 cm^{-1}, with the 944, cm^{-1} band appearing as a triplet with maxima at 938, 944 and 951 cm^{-1}. This matrix was then annealed to 33 K and recooled to 14 K and an additional spectrum recorded. All of the new, weak bands listed above (hereafter referred to as set A) grew by an factor of nearly 10, as shown in Figure 1. In addition, all of these bands grew by the same amount (i.e. they maintained a constant intensity ratio with respect to one another). A very slight reduction in parent monomer intensities was noted, and some growth in bands due to the parent CH_3OH dimer (also seen in annealed blank experiments). This annealed matrix was then irradiated for 1 h with the output of a medium-pressure Hg arc, using a Pyrex/H_2O filter, and an additional spectrum recorded. The bands of set A were greatly decreased as a result of irradiation, and new infrared absorptions appear at 676, 1129, 1150, 1425, and 1445 cm^{-1} (hereafter referred to as set B) as well as a group of bands at 2704, 2731, 2752, 2764, 2784, and 2800 cm^{-1} (set C), as shown in Figure 2. Further irradiation resulted in complete destruction of bands in set A, and some additional growth of bands in sets B and C.

(26) Gaussian 94, Revision E.1; Frisch, M. J.; Trucks, G. W.; Schlegel, H. **B**.; Gill, P. M. W.; Johnson, **B**. G.; Robb, M. A.; Cheeseman, J. R.; Keith, T.; Petersson, G. A.; Montgomery, J. A.; Raghavachari, K.; Al-Laham, M. A.; Zakrzewski, V. G.; Ortiz, J. V.; Foresman, J. **B**.; Cioslowski, J.; Stefanov, **B**. **B**.; Nanayakkara, M.; Challacombe, M.; Peng, C. Y.; Ayala, P. Y.; Chen, W.; Wong, M. W.; Andres, J. L.; Binkley, J. S.; Defrees, D. J.; Baker, J.; Stewart, J. P.; Head-Gordon, M.; Gonzalez, C.; Pople, J. A.; Gaussian, Inc.: Pittsburgh, PA, 1995.

(27) Varetti, E. L.; Muller, A. *Spectrochim. Acta* **1978**, *34A*, 895.

(28) Beattie, I. R.; Marsden, C. J.; Ogden, J. S. *J. Chem. Soc., Dalton Trans*. **1980**, 535.

(29) Barnes, A. J.; Hallam, H. E. *Trans. Faraday Soc*. **1970**, *66*, 1920.

(30) Barnes, A. J.; Hallam, H. E.; Scrimshaw, G. F. *Trans. Faraday Soc*. **1969**, *65*, 3150.

(31) Maillard, D.; Schriver, A.; Perchard, J. P. *J. Chem. Phys*. **1979**, *71*, 505.

(32) Nelander, B. *J. Mol. Struct*. **1978**, *50*, 223.

(33) Bach, S. B. H.; Ault, B. S. *J. Phys. Chem*. **1984**, *88*, 3600.

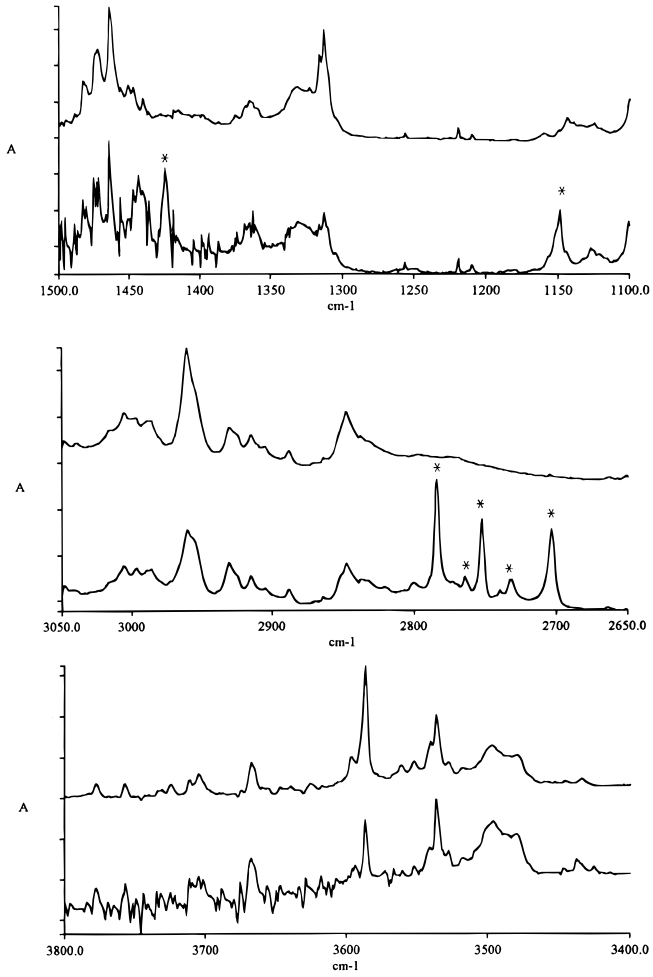

Figure 2. Infrared spectra over selected spectral regions of matrixes prepared by twin jet deposition of samples of $Ar/CrCl_2O_2 = 100$ and $Ar/CH_3OH = 250$. The lower trace was recorded after annealing and before irradiation, while the upper trace was recorded after 90 min of irradiation with a medium-pressure Hg arc, with a Pyrex/H_2O filter. Bands denoted by an asterisk are attributable to species **B** and **C**. A decrease in bands due to species A can be seen as well.

A number of twin jet experiments were conducted after this initial run. In one set of experiments, the concentrations of the two reactant samples were varied from as concentrated as 50/1 to as dilute as 500/1. In all cases, the weak product bands of set A remained, and they again grew significantly upon annealing of the matrix to between 33 and 36 K. It is noteworthy that these bands maintained a constant intensity ratio with respect one another throughout all of the experiments within uncertainty limits on the absorbances of the very weak bands.

A number of matrices were irradiated under different conditions to further explore the loss of bands in set A and the growth of bands in sets B and C. In one experiment, the wavelength dependence of photolysis was investigated. When an annealed matrix was irradiated with a medium-pressure Hg arc with use of a H_2O filter and a glass filter that only transmitted $\lambda > 600$ nm, no changes were observed in the spectrum (set A did not decrease and sets B and C did not grow in). When a glass filter was employed that transmitted $\lambda > 540$ nm, a slight decrease in sets A and a slight growth in sets B and C were noted after 130 min of irradiation. When a filter was used that transmitted $\lambda > 400$ nm, a large reduction in sets A was seen with a significant growth in sets B and C. Finally, in a separate experiment the reagents were co-deposited in the twin jet mode, and the matrix was annealed and then irradiate with the full

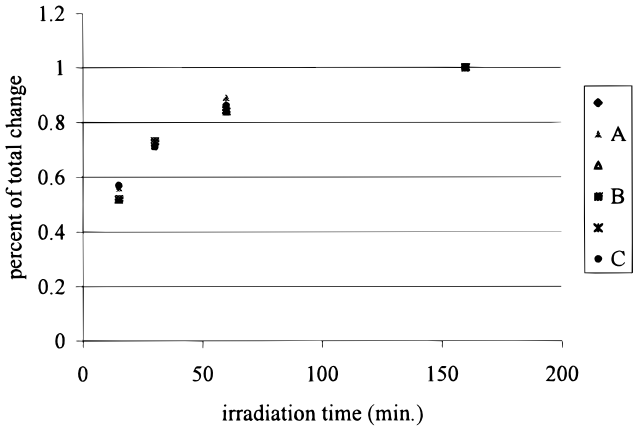

Figure 3. Irradiation time dependence of the absorptions of species **A**, **B**, and **C**, as a fraction of the total absorbance change due to irradiation. For species A, the values are the average of the four major product bands, while for species **B** and **C**, the values are the average of the three major product bands.

light of the Hg arc, using a quartz/H_2O filter that transmitted $\lambda > 200$ nm. Complete destruction of the bands in set A was noted, along with a significant growth of the bands of sets B and C. No other changes were noted in the spectrum. In all of these irradiation experiments, no changes were noted in bands due to the parent species (consistent with irradiated blank experiments).

In another experiment, an annealed matrix containing CH_3OH and $CrCl_2O_2$ was irradiated for a number of short intervals with use of the Hg arc with Pyrex/H_2O filter. In the initial 15 min irradiation period, bands in set A were reduced by approximately 50% of their original intensity, while bands of sets B and C grew to approximately 50% of their final absorbance (see below). Another 15 min irradiation period reduced set A to 25% of the original intensity, while sets B and C grew to 75% of their final intensity. Additional irradiation intervals were employed, followed by a long (120 min) interval. By the end of the irradiation intervals, set A was completely destroyed and sets B and C had reached a maximum and did not grow further. From the intensities as a function of irradiation time, a destruction curve could be constructed for set A and growth curves for sets B and C; these are shown in Figure 3.

(b) Merged Jet Experiments. These two reactants were co-deposited in the merged jet mode in a large number of experiments, employing a wide range of experimental conditions. In an initial experiment with the merged region held at room temperature and with $Ar/CrCl_2O_2 = 100$ and $Ar/CH_3OH = 500$, eight new product bands of medium intensity were observed in the resulting spectrum, at 676, 1129, 1150, 1425, 1445, 2815, 2863, and 2888 cm^{-1}, as shown in Figure 4. The first five bands match the position and relative intensities of the set B, above, while the latter three form set D. Quite intense parent bands were also observed. The overall yield of the set B bands was somewhat higher in the merged jet experiments than in the twin jet irradiation experiments. Also, the bands comprising sets A and C (above) were observed very weakly in this and all merged jet experiments. In several subsequent experiments employing the same experimental conditions, these bands were reproducible.

After these initial experiments, a number were conducted in which the concentrations of the two reactants were each varied over the range 100/1 to 500/1, again using a room-temperature merged deposition line. In these experiments, the medium intensity bands of sets B and D and the very weak bands of

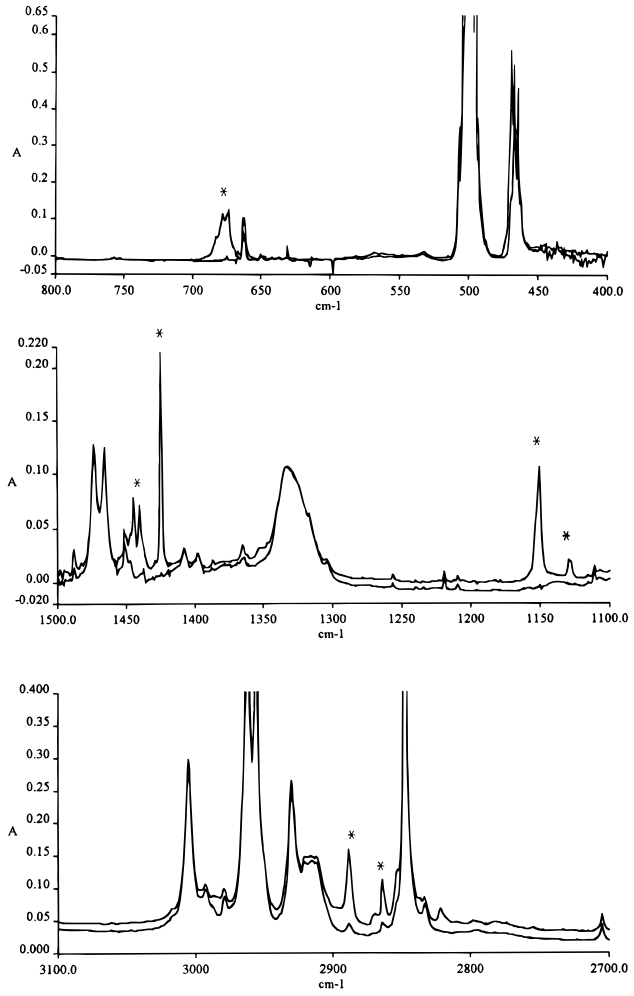

Figure 4. Infrared spectrum over selected spectral regions of a matrix prepared by twin jet deposition of samples of $Ar/CrCl_2O_2 = 100$ and $Ar/CH_3OH = 250$ (lower trace) compared to the infrared spectrum of a matrix prepared by merged jet deposition of samples of $Ar/CrCl_2O_2 = 100$ and $Ar/CH_3OH = 250$ (upper trace). The reaction zone was held at room temperature. Bands denoted by an asterisk are attributable to species B and D. Note also the absence of bands due to species C.

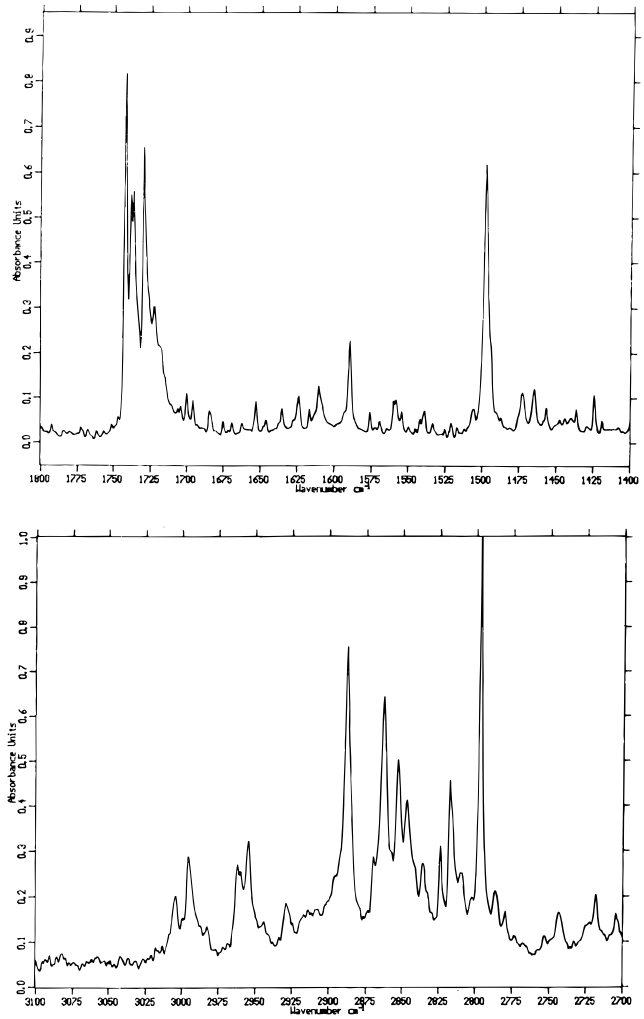

Figure 5. Infrared spectrum over selected spectral regions of a matrix prepared by merged jet deposition of samples of $Ar/CrCl_2O_2 = 100$ and $Ar/CH_3OH = 250$, with the reaction zone held at 200 °C.

sets A and C were seen reproducibly, although the absolute yield of product varied with the sample concentrations. Optimal product yield was obtained when the reactants were at a 1:1 stoichiometric ratio. Additional experiments were then conducted by using reaction zones (merged regions) of different lengths, from as short as 15 cm to as long as 300 cm. In these experiments, the same product bands (medium intensity sets B and D and very weak sets A and C) were observed with the same relative intensities. The absolute yield of the product bands was somewhat decreased but still observable with the short reaction zone while the yield of product with the 300 cm reaction zone was no greater than with the initial 125 cm reaction region. Further, no additional product bands were seen in these experiments with different lengths of the reaction zone.

A series of experiments was then conducted by using the original length (125 cm), and heating the reaction zone to increasingly higher temperatures. When the temperature of the reaction zone was held at or below 100 °C, the same product bands were observed, with approximately the same intensities. However, heating above 100 °C led to a reduction in intensity of all of the bands of sets A, B, and C; above 150 °C, these bands were completely absent from the spectrum. At the same time (above 100 °C), new bands appeared in the spectrum, near 1170, 1499, 1732, 1744, 2620, 2799, and 2855 cm^{-1} (set E), while the bands in set D increased in intensity. As the temperature of the reaction zone was increased in a subsequent experiment to 200 °C, these bands grew in intensity. In the highest yield experiments, these bands were very intense, particularly the 1744 cm^{-1} absorption, as shown in Figure 5. In addition, bands at 663, 2140, and 2344 cm^{-1} became apparent in this experiment. As the temperature of the reaction zone was increased to 250, 300, 350, and then 380 °C in an additional sequence of experiments, the bands in set E decreased in intensity and then ultimately were completely absent in the very high temperature experiments. On the other hand, the bands near 663, 2140, and 2344 cm^{-1} became very intense, with an additional band noted at 2275 cm^{-1}. Also, the set D bands grew in intensity as the temperature was increased.

(c) Isotopic Labeling Studies. To more completely identify and characterize the species responsible for new absorptions in the above experiments, $CrCl_2O_2$ was deposited with different isotopomers of CH_3OH, including $^{13}CH_3OH$, $CH_3{}^{18}OH$, CD_3OH, and CD_3OD. While isotopic purity of the commercially purchased enriched samples was 99% in the labeled element, 50% enriched samples of $^{12,13}CH_3OH$ and $CH_3{}^{16,18}OH$ were also prepared by mixing equal volumes of the natural abundance and enriched compounds. Several experiments were run with each level of enrichment of each isotopomer, both in the twin jet mode and in the merged jet mode with the 125 cm length

Table 1. Infrared Spectra and Band Assignments[a] for the 1:1 Hydrogen Bonded Complex of $CrCl_2O_2$ with CH_3OH

$^{12}CH_3{}^{16}OH$	$^{13}CH_3{}^{16}OH$	$^{12}CH_3{}^{18}OH$	$^{12}CD_3{}^{16}OH$	$^{12}CD_3{}^{16}OD$	assignment
429	429	429	429	429	Cr−Cl str
443	443	443	443	443	Cr−Cl str
944	944	944	944	944	Cr−O str (H-bonded O)
978	978	978	978	978	Cr−O str
1010		984	972	972	C−O str
1313	1306	1306	1253	784	C−O−H bend
			1105	1105	CH_3 def
3591	3591	3580	3591	2655	O−H str

[a] Band positions in cm^{-1}.

Table 2. Infrared Spectrum and Band Assignments[a] for $ClCrO_2OCH_3$

$^{12}CH_3{}^{16}OH$	$^{13}CH_3{}^{16}OH$	$^{12}CH_3{}^{18}OH$	$^{12}CD_3{}^{16}OH$	$^{12}CD_3{}^{16}OD$	assignment
676	671	662	652	652	Cr−O str
1129	1122	1123			CH3 rock
1151	1143	1144			CH3 rock
1425	1421	1423	1054	1054	CH3 def
1443	1440	1442	1081	1081	CH3 def
			2176	2176	CH3 def

[a] Band positions in cm^{-1}.

reaction zone. The twin jet experiments paralleled closely those conducted with normal isotopic CH_3OH, above. For each isotopomer, a set of weak absorptions was noted upon initial deposition, analogous to set A, and are listed in Table 1. These were observed to grow markedly upon sample annealing to 34 K and were destroyed by Hg arc irradiation. New bands counterpart to set B were observed to grow in upon irradiation, with shifts in band position as a result of isotopic labeling. The isotopic set B bands are listed in Table 2. The set C bands formed upon irradiation did *not* show any shifts when $^{13}CH_3OH$, $CH_3{}^{18}OH$ or CD_3OH was employed. However, when CD_3OD was employed, counterpart bands were observed at 1961, 1980, 1997, 2003, 2019, and 2027 cm^{-1}.

In the merged jet experiments with the reaction region held at room temperature, counterpart bands were observed to those observed in the natural abundance experiments. The set B bands at 676, 1129, 1150, 1425, and 1445 cm^{-1} showed distinct isotopic shifts as are listed in Table 2, again identical to the bands that grew in as a result of irradiation in the twin jet experiments. When 50% mixtures of $^{12,13}C$ and $^{16,18}O$ isotopomers were employed in different experiments, the bands at 676, 1129, 1150, and 1425 cm^{-1} each appeared as clear, distinct doublets, with peaks at positions matching the pure ^{12}C, ^{13}C, ^{16}O, and ^{18}O isotopic experiments. The bands in set D showed no shift with ^{13}C, ^{18}O, or $-CD_3$ substitution, but did shift with $-OD$ substitution, to near 2100 cm^{-1}.

Experiments employing these different isotopomers were also conducted while heating the reaction zone to 150, 200, 250, and 350 °C. A pattern similar to the natural abundance isotopic experiments was observed: the bands of sets A, B and C were destroyed by heating above 150 °C, and new product bands grew in as isotopic counterparts to the set E bands. In the 50% $^{12,13}C$ and $^{16,18}O$ experiments, each of these bands appeared as a distinct isotopic doublet. These are listed in Table 2. On the other hand, the band at 2620 cm^{-1} and the set **D** bands did not shift with ^{13}C and ^{18}O isotopic labeling. However, when CD_3OH was employed, the set D bands shifted to near 2100 cm^{-1} and the 2620 cm^{-1} band shifted to 1916 cm^{-1}. Above 250 °C, the set E bands were themselves destroyed, and bands counterpart to the 663, 2140, and 2344 cm^{-1} high-temperature bands described above grew in. The 663 and 2344 cm^{-1} bands appeared as doublets in the mixed $^{12,13}C$ experiments and triplets in the mixed $^{16,18}O$ experiments.

$CrCl_2O_2$ + CH_2O. Formaldehyde is a likely intermediate oxidation product of CH_3OH, and may itself be oxidized further. To explore this possibility, CH_2O was sublimed from solid paraformaldehyde and passed through the reaction zone with samples of $Ar/CrCl_2O_2 = 100$. When CH_2O and $CrCl_2O_2$, diluted in argon, flowed together through the reaction zone held at 160 °C, no new bands were observed in the spectrum while very intense bands due to CH_2O and $CrCl_2O_2$ were noted. When similar experiments were conducted with the reaction zone at 330 °C, all of the bands of parent $CrCl_2O_2$ and CH_2O were absent, and strong new bands were observed at 663, 2140, and 2344 cm^{-1}, as well as a multiplet of bands between 2800 and 2900 cm^{-1}. In a final experiment, CH_2O and $CrCl_2O_2$ were reacted at the intermediate temperature of 240 °C. In this experiment, some reduction of parent band intensities was noted, along with some growth of the bands at 663, 2140, and 2344 cm^{-1}, although not nearly to the same intensity as in the 330 °C experiments.

$CrCl_2O_2$ + HCl. In one experiment, a sample of $Ar/HCl = 250$ was co-deposited with a sample of $Ar/CrCl_2O_2 = 100$ in the merged jet mode to look for possible interactions between these two species. Only a single new absorption, at 2837 cm^{-1}, was noted in this experiment after comparison to a comparable blank experiment of $Ar/HCl = 250$.

Discussion

Numerous product bands and several product species were isolated in the reaction of $CrCl_2O_2$ with CH_3OH under a range of reaction conditions. As noted above, many of the product bands can be grouped into sets, based on the conditions under which they appeared, and the fact that bands within a given set maintained a constant intensity ratio with respect to other bands in that set. It is also apparent that the different product species are formed in sequence, as reaction conditions are altered and additional energy deposited into the system. The identity of the species responsible for each set of product bands will be discussed, followed by the results of ab initio calculations and an overview of the mechanism of reaction.

Product Identification. The bands in set A were formed under the conditions of shortest reaction time and lowest reaction temperature, namely in the twin jet deposition experiments where mixing of the two reactants occurs on the surface of the condensing matrix. This indicates the species **A** is the initial

intermediate in the reaction between $CrCl_2O_2$ and CH_3OH. Further, while the yield of species **A** was quite low during deposition, species **A** was produced in significant amounts by annealing the matrix to 33 K. Thus, the barrier to formation of **A** from the isolated reactants must be very low. This is indicative of the formation of a molecular complex between the two subunits.[34] Spectroscopically, this would be manifested by a shifting of certain vibrational modes of the two subunits, particularly modes involving atoms at the site of complexation. In addition, since CH_3OH is known to serve as a proton donor in hydrogen bonding interactions and $CrCl_2O_2$ has four very electronegative ligands, hydrogen bond formation is reasonable. Spectroscopically, the three vibrational modes of the CH_3OH subunit most perturbed by the formation of the complex were the O−H stretch (shifted from 3667 cm^{-1} in the parent to 3591 cm^{-1} in the complex), the C−O−H bend, and the C−O stretch as shown in Table 1. These observations, particularly the distinctly red-shifted hydrogen stretching mode, are consistent with hydrogen bond formation.[35] Also shifted to lower energy is one of the C═O stretching modes of $CrCl_2O_2$ (from 990 cm^{-1} in the parent to 944 cm^{-1} in the complex) as well as the two Cr−Cl stretching modes. Finally, detailed ab initio calculations by Ziegler et al. concluded that the initial product in this system is a hydrogen bonded complex.[18] All of these observations point to the identification of species **A** as a hydrogen bonded complex between CH_3OH and $CrCl_2O_2$, the initial intermediate for this pair of reactants. Band assignments for this hydrogen bonded complex are given Table 1.

The initial complex was destroyed by Hg arc irradiation while trapped in the cryogenic matrix, giving rise to the bands in sets B and C. *Set B was also formed in the room-temperature merged jet reaction of $CrCl_2O_2$ with CH_3OH*, accompanied by the production of bands in set D. The bands in set D can be readily assigned to matrix isolated HCl by comparison to authentic matrices containing HCl, as well as to the literature. This is consistent with a lack of ^{13}C and ^{18}O shift and a strong deuterium shift for these bands. The bands in set **C** showed similar isotopic behavior to HCl, with a lack of ^{13}C and ^{18}O shift, and a strong deuterium shift. Specifically, the H/D frequency ratio for each band of species C is 1.38, exactly the ratio observed for HCl in the gas phase[36] and in argon matrixes.[30,31] However, the bands in set C were approximately 100 cm^{-1} to lower energy of matrix-isolated HCl, suggesting that they are due to hydrogen bonded HCl. From the growth curves as a function of irradiation time (Figure 3), set C is produced at the same time and at the same rate as set B, and they both arise from the photodestruction of the initial hydrogen bonded complex (species **A**). Thus, species **B** and species **C** are very likely trapped within the same matrix cage. If HCl is formed in the photoreaction, then it would be expected to form a hydrogen bond with species **B**. In the thermal, merged jet reaction the HCl that is produced is able to separate from species **B** in the gas phase prior to matrix deposition, and is trapped primarily as free HCl. Thus, species **D** is identified as free, matrix-isolated HCl while species **C** is identified as HCl weakly hydrogen bonded to species **B**.

Species **B** must arise from the photodestruction of species **A** and the concomitant production of HCl. It is noteworthy that when CD_3OH was employed, DCl was not a product in either the thermal, merged jet reaction or the photochemical twin jet reaction. DCl was produced only when CD_3OD was employed. This demonstrates that the −OH group leads to HCl production (or −OD to DCl formation). The second fragment arising from HCl elimination would be $ClCrO_2OCH_3$, a species analogous to parent chromyl chloride but with a methoxy group replacing one chloride ligand. Chemically, one might anticipate that this species should be stable and the calculations of Ziegler et al. did find an energy minimum for this species,[16] as did earlier calculations by Goddard and co-worker.[14] $ClCrO_2OCH_3$ has four quite electronegative ligands, three of which are different, providing multiple sites for hydrogen bonding to the HCl that is produced photochemically in the same cage (species **C**). Also, the observation of distinct doublets when 50−50 mixtures of $^{12}CH_3OH/^{13}CH_3OH$ and $CH_3{}^{16}OH/CH_3{}^{18}OH$ were used demonstrates that the product species contains 1 carbon atom and 1 oxygen atom (from the methanol reactant), consistent with addition of a methoxy ligand to the chromium center. In addition, ab initio calculations on $ClCrO_2OCH_3$ described below predict very well the infrared spectrum observed for species **B**, particularly the isotopic shifts of the Cr−O stretch of the methoxy ligand. ***Thus, species B is identified as the HCl elimination product of the initial hydrogen bonded complex, $ClCrO_2OCH_3$.*** As will be discussed below, this conclusion is not fully consistent with the calculations of Ziegler which suggest that the hydrogen shift product, $Cl_2CrO(OH)OCH_3$, is the second intermediate in the reaction pathway, but is consistent with the calculations of Goddard et al. Band positions and assignments for $ClCrO_2OCH_3$ are collected in Table 2.

While the photochemical reaction producing species **B** and **C** did not lead to additional products, heating the reaction zone in the merged jet experiments did lead to further reaction. Above approximately 150 °C, bands due to species **B** were destroyed and intense bands due to species **D** and **E** grew in. Species **D**, as noted above, is identified as HCl, while the bands of species **E** are readily assigned to CH_2O and the complex of CH_2O with HCl, by comparison with authentic samples and with the literature.[32,33] Further, the isotopic shifts of the bands in set E matched exactly the known bands of CH_2O. It is also important to note that when CD_3OH was employed, a high yield

Table 3. Optimized Structures

$Cl_2CrO(OH)OCH_3$		$ClCrO_2OCH_3$	
parameter	B3LYP/6-311g* [a]	parameter	B3LYP/6-311g* [a]
R(Cr−Cl)	2.205	*R*(Cr−Cl)	2.147
R(Cr−Cl)	2.305	*R*(Cr═O)	1.554
R(Cr═O)	1.529	*R*(Cr═O)	1.551
R(Cr−O)	1.787	*R*(Cr−O)	1.720
R(O−H)	0.966	*R*(C−O)	1.424
R(Cr−O)	1.729	*R*(C−H)	1.094
R(O−C)	1.405	*R*(C−H)	1.093
R(C−H)	1.098	*R*(C−H)	1.091
R(C−H)	1.097	*a*(O═Cr═O)	110.4
R(C−H)	1.090	*a*(O═Cr−Cl)	109.0
a(Cl−Cr−Cl)	85.9	*a*(O═Cr−Cl)	110.3
a(Cl−Cr═O)	110.6	*a*(Cl−Cr−O)	109.4
a(Cl−Cr═O)	96.7	*a*(O═Cr−O)	109.4
a(Cl−Cr−O)	135.4	*a*(O═Cr−O)	109.2
a(Cl−Cr−O)	82.4	*a*(Cr−O−C)	127.0
a(O═Cr−O)	113.5	*a*(O−C−H)	110.1
a(O═Cr−O)	103.0	*a*(O−C−H)	110.0
a(Cr−O−H)	117.1	*a*(O−C−H)	107.5
a(Cl−Cr−O)	90.8		
a(C1−Cr−O)	159.9		
a(Cr−O−C)	127.4		
a(O−C−H)	109.3		
a(O−C−H)	108.2		
a(O−C−H)	108.3		

[a] This work.

(34) Ault, B. S. *Rev. Chem. Intermed.* **1988**, *9*, 233.
(35) Pimentel, G. C.; McClelland, A. L. *The Hydrogen Bond;* W. H. Freeman: San Francisco, 1960.
(36) Nakamoto, K. *Infrared and Raman Spectra of Inorganic and Coordination Compounds*, 5th ed.; Wiley-Interscience: New York, 1997.

Table 4. Comparison of Calculated[a] and Experimental Band Positions[b] for $ClCrO_2OCH_3$ and $Cl_2CrO(OH)OCH_3$

		band position		^{13}C shift		^{18}O shift		CD_3 shift	
molecule	mode	exptl	calcd	exptl	calcd	exptl	calcd	exptl	calcd
$ClCrO_2OCH_3$	Cr−O stretch	676	684	−5	−5	−14	−15	−24	−22
	CH_3 rock	1129	1127	−7	−8	−6	−3	not observed	
	CH_3 rock	1151	1143	−8	−8	−7	−5	not observed	
	CH_3 deformation	1425	1435	−4	−5	−2	−2	−344	−342
	CH_3 deformation	1443	1447	−3	−1	−1	0	−389	−402
$Cl_2CrO(OH)OCH_3$	Cr−O stretch	676	620	−5	−3	−14	−8	−24	−22
	CH_3 rock	1129	1091	−7	−8	−6	−4	not observed	
	CH_3 rock	1151	1147	−8	−9	−7	−7	not observed	
	CH_3 deformation	1425	1393	−4	−4	−2	−2	−371	−395
	CH_3 deformation	1443	1432	−3	−4	−1	−3	−362	−407

[a] Calculated using density functional theory, with theB3LYP functional and the 6-311 g* basis set. [b] Band positions in cm^{-1}.

of DCl was formed, and the complex of DCl with CD_2O.[33] This result is in agreement with earlier experimental work and with ab initio calculations. When the reaction zone was heated above 250 °C, bands due to CH_2O decreased in intensity and strong bands grew in at 663, 2150, and 2344 cm^{-1}. These are readily assigned to CO and CO_2, as well as the appropriate isotopomers in the isotopic labeling experiments. Finally, when CH_2O was sublimed directly into the reaction zone of the merged jet system and reacted with $CrCl_2O_2$ above 250 °C, bands due to CH_2O diminished in intensity and the bands due to CO and CO_2 became very intense.

***Ab Initio* Calculations.** Hartree−Fock and density functional (DFT) calculations were carried out in support of the experimental results, using the 3-21G* and 6-311G* basis sets; the B3LYP functional was used for the DFT calculations.[25] On the basis of previous work, $ClCrO_2OCH_3$ and $Cl_2CrO(OH)OCH_3$ were the two species most likely to be identified as species **B**. Both of these species optimized to stable minima; the structure found for $Cl_2CrO(OH)OCH_3$ was quite similar to that calculated by Ziegler et al. using density functional theory. The optimized structure for $ClCrO_2OCH_3$ was relatively similar, as shown in Table 3. Harmonic vibrational frequencies were then calculated at both the RHF and DFT levels of theory and compared to the observed spectrum of species **B**, including all isotopomers. While only five bands were observed for species **B**, the fit was overall better for $ClCrO_2OCH_3$. Both species are predicted to have a Cr−O−C stretching mode in the 600−700 cm^{-1} range in the DFT/6-311G* calculation. The position and all of the isotopic shifts clearly identify the band at 676 cm^{-1} in the merged jet experiments as this mode. The unscaled DFT/6-311G* calculation puts this mode at 705 cm^{-1} while for $Cl_2CrO(OH)OCH_3$ this mode is calculated at 639 cm^{-1}, *below* the experimental value. While no widely accepted scaling factor has been adopted for B3LYP/6-311G*, a value around 0.97 is a reasonable estimate given accepted scaling factors for B3LYP with other basis sets (e.g. 0.961 for the 6-31G* basis set[37]). A value slightly less than 1.00 is anticipated, based on the harmonic approximation built into the calculation. Thus, as shown in Table 4, the scaled value for $ClCrO_2OCH_3$ is 684 cm^{-1} while for $Cl_2CrO(OH)OCH_3$ the scaled value is 620 cm^{-1}, substantially lower than the experimental value. The fit to the other observed bands of species **B** was also distinctly better for $ClCrO_2OCH_3$ than for $Cl_2CrO(OH)OCH_3$. In addition, additional intense bands are calculated for $Cl_2CrO(OH)OCH_3$ in spectral regions that are not congested (e.g. the O−H stretch of the hydroxyl group); these bands were not observed. While additional bands are also calculated for $ClCrO_2OCH_3$, they are fewer in number (due to the smaller number of atoms in the molecule); those that are calculated to have substantial intensity fall very close to intense parent bands of CH_3OH and $CrCl_2O_2$ and may well be obscured.

Calculations were also carried out at the same level (B3LYP/6-311G*) for CrO_2, HCl, and CH_2O, to evaluate the energetics of the different species and the possible decomposition pathways of $ClCrO_2OCH_3$ and $Cl_2CrO(OH)OCH_3$. These calculations parallel those done by Ziegler and by Goddard, but with a different set of functionals. The present calculations indicate that $ClCrO_2OCH_3$ is energetically more stable than $Cl_2CrO(OH)OCH_3$ by approximately 19 kcal/mol, in qualitative agreement with findings of Ziegler and Goddard. The calculations further indicate that there is a large barrier, slightly greater than 100 kcal/mol, to the decomposition of $ClCrO_2OCH_3$ to CrO_2, HCl, and CH_2O. This is in reasonable agreement with the barrier calculated by Ziegler of +92 kcal/mol.[18]

Mechanistic Inferences. A series of intermediates have been suggested over the years to explain the role of $CrCl_2O_2$ in the oxidation of CH_3OH and other organic substrates. The earlier calculations of Goddard et al. proposed specific intermediates and the recent calculations of Ziegler et al. extended this work. Ziegler in particular identified the initial intermediate as a hydrogen bonded complex,[18] experimentally observed for the first time in the present study as species **A**. Both Ziegler and Goddard identified $Cl_2CrO(OH)OCH_3$ and $ClCrO_2OCH_3$ as potential second intermediates; both concluded that O−H bond addition was energetically favorable to C−H bond addition. Goddard calculated the latter species to be slightly lower in energy than the former, as did Ziegler. These calculations are consistent with the identification here of species **B** as $ClCrO_2OCH_3$. While lower in energy, Ziegler et al. concluded that $ClCrO_2OCH_3$ was *not* an active intermediate in the oxidation of CH_3OH due to the substantial endothermicity they calculated[16] for the dissociation of this species into CH_2O, HCl, and CrO_2. As noted above, the present calculations reproduce this substantial endothermicity. In the present study, species **B** clearly decomposed or was consumed at temperatures above 150 °C; the loss of **B** was clearly accompanied by the formation of both CH_2O and HCl. It is also important to note that when CD_3OH was used as the starting material, formation of species **B** was accompanied by formation of DCl. This demonstrates that the HCl formed in this step arises from the methyl group of the parent methanol. The mechanism of decomposition of $ClCrO_2OCH_3$ to HCl, CH_2O, and (presumably) CrO_2 is not clear in view of the large endothermicity of the gas-phase reaction. One reasonable explanation is that the decomposition of species **B** at elevated temperatures is surface-mediated by the walls of

(37) Foresman, J. B.; Frisch, A. E. *Exploring Chemistry with Electronic Structure Methods*; Gaussian, Inc.: Pittburgh, PA, 1996; and references therein.

the deposition system. Under these conditions, the calculations and experiments cannot be compared, since the calculations are for isolated, gas-phase species and reactions. In any event, the experimental work and present *ab initio* calculations argue for the identification of species **B** in these experiments as $ClCrO_2OCH_3$, and this species is destroyed at elevated temperatures as CH_2O and HCl are produced.

Conclusions

Twin jet and merged jet matrix isolation experiments led to the formation of a series of intermediate products in the oxidation of CH_3OH by $CrCl_2O_2$. Initially formed was a 1:1 hydrogen bonded complex, a species that further reacted at room temperature to eliminate HCl and produce $ClCrO_2OCH_3$. This reaction could also be induced by visible irradiation of the hydrogen bonded complex trapped in an argon matrix. Pyrolysis above 150 °C of $ClCrO_2OCH_3$ in a flowing gas reactor followed by matrix trapping led to destruction of this species, and the production of CH_2O in high yield. This species, in turn, could be oxidized further by $CrCl_2O_2$ to CO and CO_2 at temperatures above 250 °C.

Acknowledgment. The National Science Foundation is gratefully acknowledged for partial support of this research through Grant No. CHE 93-22622.

JA9808752